Article

Design and Development of Instrumented Toys for Social Interactive Assessment of Infant Cognitive Flexibility

Vishal Ramanathan[1], Mohammad Zaidi Ariffin[1], Goh Guo Dong[2], Goh Guo Liang[3], Mohammad Adhimas Rikat[3], Tan Xing Xi[4], Yeong Wai Yee[2], Juan-Pablo Ortega[6], Victoria Leong[4,5], Domenico Campolo[1]*

[1] Robotics Research Center, School of Mechanical and Aerospace Engineering, Nanyang Technological University, Singapore
[2] Singapore Centre for 3D Printing, School of Mechanical and Aerospace Engineering, Nanyang Technological University, Singapore
[3] School of Mechanical and Aerospace Engineering, Nanyang Technological University, Singapore
[4] Psychology, School of Social Sciences, Nanyang Technological University, Singapore
[5] Department of Pediatrics, University of Cambridge, Cambridge, UK
[6] Division of Mathematical Sciences, Nanyang Technological University, Singapore
* Correspondence: d.campolo@ntu.edu.sg; Tel.: +65-6790-5610

Abstract: The first years of an infant's life represent a sensitive period for neurodevelopment and see the emergence of nascent forms of executive function (EF), which are required to support complex cognition. Few tests exist for measuring EF during infancy, and the available tests require painstaking manual coding of infant behaviour. In modern clinical and research practice, human coders collect data on EF performance by manually labelling video recordings of infant behaviour during toy or social interaction. Besides being extremely time-consuming, video annotation is known to be rater-dependent and subjective. To address these issues, starting from existing cognitive flexibility research protocols, we developed instrumented toys as a new task instrumentation and data collection tool suitable for infant use. A commercially available device comprising a Barometer and Inertial Measurement Unit (IMU) embedded in a 3D-printed lattice structure was used to detect when and how the infant interacts with the toy. The data collected using the instrumented toys provides a rich dataset describing the sequence of toy interaction and individual toy interaction patterns, from which EF-relevant aspects of infant cognition may be inferred. Such a tool potentially provides an objective, reliable, and scalable method of collecting early developmental data in socially interactive contexts.

Keywords: Instrumented Toys; Ecological Behavioural Assessment; Executive Function Development; Inertial Motion Detection; Barometric Force Sensing; 3D Printing

1. Introduction

Executive Functions (EFs) are higher-order cognitive control mechanisms commonly conceptualised as a triad of mental skills comprising inhibitory control, working memory and cognitive flexibility [1]. These mental abilities support complex thinking skills such as reasoning and creative problem-solving [2] and influence the development of socioemotional competencies such as the Theory of Mind [3]. They are considered essential for mental and physical health [4–6].

Cognitive flexibility refers to switching between tasks, rules or dimensions and adapting one's behaviour to a changing environment [7,8]. Categorisation tasks test an infant's ability to flexibly categorise objects based on different dimensional features (or attentional sets) such as shape versus material [9,10]. An infant's mental categorisation of objects can be inferred from a behavioural measure of sequential touching. If infants sequentially touch objects from the same category (e.g. balls) more often than expected by chance, it is inferred that they are doing so because they perceive these objects to belong to the same category [11–13] (Figure 1). Horst and colleagues (2009) [14] found that 14-18-month-old infants could

Preprints (www.preprints.org) | NOT PEER-REVIEWED | Posted: 29 December 2022 doi:10.20944/preprints202212.0554.v1

flexibly adapt their categorisation of objects by either a perceptually salient dimension of taxonomic distinction (e.g. shape) or a less salient dimension (e.g., deformability).

Figure 1. Example of infant performing object categorisation task. (Image used with specific parental consent.)

Changes in the pattern of an infant's object touch sequences can index mental set-shifting, i.e. shifts in the mental dimensional set that infants use for categorisation, such as shape or compressibility. Further, it is possible to measure the effect of maternal scaffolding on infant mental set-shifting via the introduction of a brief period of maternal social interaction during which she demonstrates object compressibility to the infant. However, to detect sequences of object touches made by infants and the quantification of maternal behaviour during this period of social interaction, these events must first be manually extracted and coded from video footage by a trained human coder.

One common performance measure is Mean Run Length (MRL), where run lengths are the number of touches in a row to objects from the same category (i.e., shape). MRLs are calculated by dividing the total number of touches by the total number of runs across all categories [15]. The calculated MRLs are then compared against a Monte-Carlo simulation's average "random" sequence lengths to assess performance against chance [14]. In addition to these classic measures, newer indices based on the conditional probability of infant touch sequences may provide further insight into the cognitive strategies adopted by infants during this task.

This paper presents a set of instrumented toys as an objective, reliable, and scalable form of cognitive flexibility task instrumentation and behaviour measurement tool that can complement and accelerate manual means of data coding. It can extract typically coded measures such as - when a toy is touched, how long the infant interacts with it, and the overall touching sequence. We can additionally measure squeezing patterns the infants' exhibit to validate mental set-shifting from shape-based to material-based categorisation.

2. Functional, Technical, and Physical Specifications

2.1. Requirements and Existing Setup

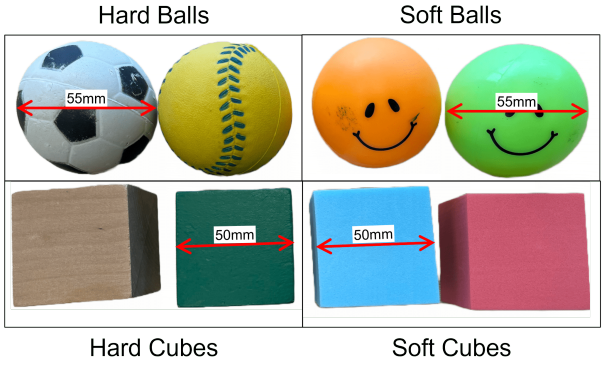

Figure 2. Example of toys used in object categorisation task.

Preprints (www.preprints.org) | NOT PEER-REVIEWED | Posted: 29 December 2022 doi:10.20944/preprints202212.0554.v1

To evaluate mental set-shifting in infants during the object categorisation task, the number and sequence of touches of each object by the infant need to be identified. The current methodology relies on human coders manually extracting these touch sequences by watching video recordings of infants playing with toys. The set of 8 toys comprises 2 hard balls (79 g), 2 soft balls (23 g), 2 hard cubes (80 g), and 2 soft cubes (5 g)(Figure 2). All the cubes have sides measuring 50 mm, and all the spheres have diameters measuring 55 mm and are all different colours. A latent factor currently not measured that could be useful in reinforcing the identification of mental set-shifting in infants based on the less salient dimension of deformability would be to measure the squeezing patterns of the infant's grasp on the toys.

2.2. Detecting Toy Interaction

To scale up the object categorisation task for lab-based and ecological environments, we need to automatically detect when and how an infant interacts with the toys. Motion tracking enables the desired automatic extraction of interaction and motion patterns. It can be implemented using various technological solutions, as shown in [16]. However, not all solutions are suitable for use in ecological environments. We also need to keep costs low while being easy to set up and manage. Based on technological assessments to identify suitable techniques for motion tracking, optical and inertial sensing seem to be the most favourable and widely used [17,18].

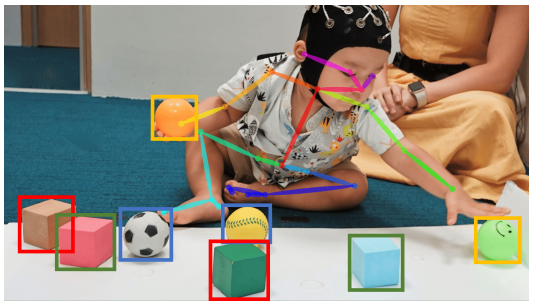

Figure 3. Computer Vision based pose detection and object tracking. (Image used by specific parental consent.)

Optical marker-less methods can be used on recorded videos that are part of the existing object categorisation task paradigm. Combining Human Pose Detection, Object Detection, and Multi Object Tracking algorithms, key points can be detected and tracked throughout the video (Figure 3) [18–20]. However, the accuracy of the underlying detection algorithms determines the performance, which suffers from the issue of occlusions. It also requires a structured environment restricted to the area within the camera's field of view.

Alternatively, Inertial measurement unit (IMU) based motion and orientation tracking eliminates line of sight problems and structured environment requirements making it more appealing from an ecological perspective. They are a compact, low-cost and robust way to detect the motion and orientation of objects. They have been extensively used in lab-based and ecological studies of infant motor development [21–23] and are the ideal method to detect motion and interaction for our application.

2.3. Detecting Toy Squeezing

To detect the squeezing of the toys, we need to detect the forces applied to them using force, pressure or tactile sensors. Several different working principles for such sensors were explored by [24–26] and have been used in previous infant-related research. A sensorised ball designed by Campolo et al. [27] used Quantum Tunneling Composites (QTC), which change its electrical resistance based on changes in applied force [28], to detect grasping patterns during manipulation. Cecchi et al. [29] incorporated piezoresistive pressure sensors and flexible Force Sensing Resistors (FSR) sensors in sensorised toys to measure infants' reaching and grasping. Serio et al. [30] use pressure sensors connected to air

 doi:10.20944/preprints202212.0554.v1

chambers to measure the amplitude of the force applied for quantitative monitoring and measuring infants' motor development.

Tenzer and Jentfot [31,32] developed a versatile, low-cost, and sensitive tactile sensor using commercial off-the-shelf MEMS barometers and commercialized it as TakkTile [33]. It has been used in robotics by Ades et al. [34], and Koiva et al. [35] to sense grasping events using robotic grippers. The working principle of the MEMS barometer-based tactile sensor is the communication of surface contact pressure within a layer of rubber to the ventilation hole of the sensor and, thus, to the MEMS transducer. Similarly, Takada et al. [36] and Quinn et al. [37] have used a waterproof mobile device's built-in barometer to measure touch force. It also works on a similar principle. When an airtight or waterproof device is touched, the distorted surface changes the air pressure inside that device and thus changes the built-in barometer value [36,37]. This ability to detect forces through changes in internal pressure makes barometric tactile sensing suit our requirements for a low-cost, versatile, and sensitive way to detect squeezing forces on the toy.

2.4. Proposed Platform

For the object categorisation task, balls and cubes help assess an infant's cognitive flexibility. The selected sensors need to be integrated into a platform that can be used with minimal alterations to existing paradigms. We propose the use of instrumented toys to measure the development of EF in infants in a scalable manner in lab-based and ecological environments.

Campolo et al. [27] designed a sensorised ball to analyse the development of perceptual and motor still in ecological environments. IMUs have been embedded in toys to assess spatial cognition [21,22,38] and detect possible autism spectrum disorders (ASD) at an early stage [23]. Pressure and force sensors were used to study infants' grasping actions [29,30,39]. A whole suite of instrumented toys was developed to provide early intervention for infants at risk for neurodevelopmental disorders and reduce parental stress [40,41].

These examples demonstrate the viability of instrumented toys for integrating sensors to assess infant development. However, instrumented toys specifically targeted at measuring the development of EF in infants are yet to be developed, and a need exists for such tools.

3. Instrumented Toy Design and Fabrication

3.1. Sensor Core

Using commercially available sensors, particularly in infant behavioural research tool development, has the advantage of being certificated for public use while ensuring high quality and safety standards are met. These certifications reduce the potential risk of harm when using instrumented toys that contain sensors and batteries in particular. It allows us to leverage existing expertise in sensor development while focusing on the design, development and deployment of instrumented toys at scale without compromising accuracy.

Figure 4. MindMaze Physilog 6® (P6) Sensor.

 doi:10.20944/preprints202212.0554.v1

We use Physilog 6® (P6), a commercial off-the-shelf sixth-generation wearable motion sensor platform produced by MindMaze Assessments (Figure 4). It comprises a 9 Degree-of-Freedom Inertial Measurement Unit (IMU) and Barometer typically used for human motion and gait analysis [42,43]. Its versatility allows us to capture, measure, and analyse the necessary parameters for detecting the touching and squeezing of toys during the object categorisation task.

Table 1. MindMaze Physilog 6® (P6) Specifications [44].

Dimensions	42.2 mm x 31.6 mm x 15 mm
Weight	15 g
IP Rating	Waterproof IP64
Interface	High-speed USB 2.0 USB-C connector
Wireless Communication	Bluetooth Low Energy (BLE)
Battery	240 mAh Lithium-Ion Polymer accumulator
Battery Life	up to 20 hours
Inertial Sensors	3D Accelerometer up to ±16 g 3D Gyroscope up to ±2000/s Sampling frequency up to 512 Hz
Magnetic field sensor	3D magnetic field sensor up to ±50 mT Sampling frequency up to 256 Hz
Ambient Sensor	Barometric altitude from 26 to 126 kPa Temperature sensor accuracy of ±1.5C Sampling frequency up to 64 Hz

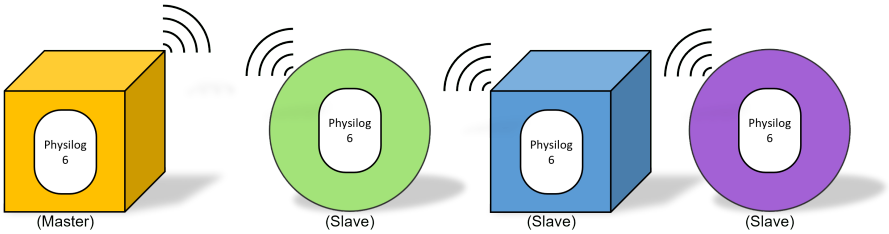

Figure 5. BLE based communication for P6 sensor data synchronisation.

Each instrumented toy will have a P6 sensor embedded to detect the touching and squeezing of the toys. The specifications of the P6 sensor are summarised in Table 1. The IMU and barometer were configured to sample at 64 Hz for easy data synchronisation, maximising battery life while striking a suitable temporal resolution. The P6 sensor has an internal clock that can be synchronised to a PC's clock, which allows for easy synchronisation with other sensors opening up the possibility of multi-modal data analysis for studying EF development. Multiple P6 sensors can communicate and synchronise with each other using the built-in BLE communication protocol. One sensor acts as the master, wirelessly broadcasting the clock signal on a particular channel, and the others act as the client listening to this signal (Figure 5). Data stored onboard as ".BIN" files are sorted into timestamped folders accessed by connecting the sensor to a PC via the USB-C interface and downloading it.

Preprints (www.preprints.org) | NOT PEER-REVIEWED | Posted: 29 December 2022 doi:10.20944/preprints202212.0554.v1

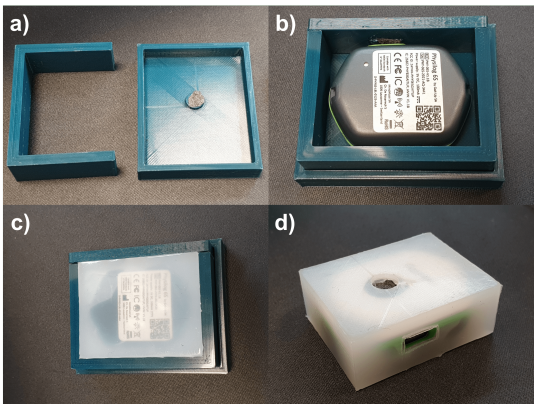

Figure 6. Sensor core with P6 sensor encased in silicone.

Dragon Skin™ 20, a high-performance platinum cure liquid silicone compound, was used to seal the hole of the P6 sensor's barometer to use it as a tactile sensor. The silicone will transduce the squeezing forces on the surface to changes in internal pressure that the barometer can detect. A custom 3D printed mould (Figure 6(a,b)) was used to enclose the sensor and shape the silicone layer surrounding it. The silicone was cured overnight Figure 6(c) and unmoulded to create the final sensor core for the instrumented toys Figure 6(d).

3.2. Physical Structure

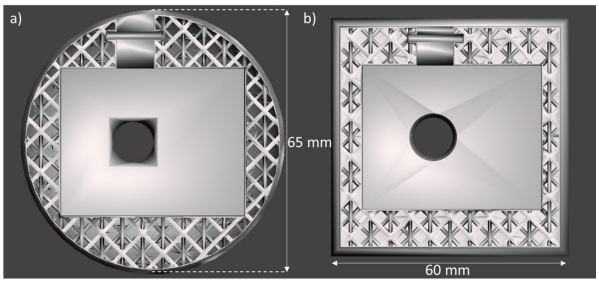

Figure 7. Lattice structure with different outer geometries. a) sphere b) cube).

The physical structure of the instrumented toy encloses the sensors, creates the final shape, and controls the rigidity. The weight and dimensions of the physical structure of the instrumented toys were defined by the anthropometry of an infant's hand, the existing regular toys used, and the physical dimensions of the sensor (44 mm x 36 mm x 17 mm) to be embedded. The cube has a length of 60 mm, and the sphere has a diameter of 65 mm.

Modern 3D printing technologies and advances in material science have enabled the fabrication of complex structures using materials of varying rigidity [45–48]. Ansys SpaceClaim's Faceted Shell and Infill tool was used to design an octahedral lattice that minimises mass, ensures uniform stiffness, and avoids needing a support structure during fabrication. The lattice structure was designed with a wall thickness of 1 mm, a unit cell size of 10 mm, and a strut thickness of 1 mm, which translates to 11% infill density (Figure 7).

Table 2. Print parameters for the fabrication of lattice structures.

	Nozzle temperature	Bed Temperature	Print Speed	Layer Thickness
TPU (85A/95A)	235°C	50°C	30 mm/s	0.2 mm

Fused Deposition Modeling (FDM) 3D printing using Thermoplastic Polyurethane (TPU) filament was used to fabricate the octahedral lattice physical structure (Figure 8).

 doi:10.20944/preprints202212.0554.v1

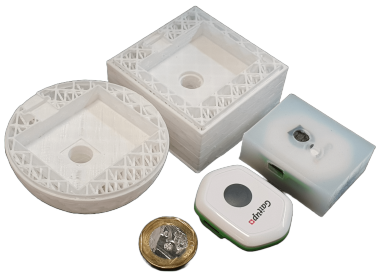

Figure 8. 3D printed lattice structure design prototype.

The hard toys were printed using a 95A shore hardness TPU filament, while the soft toys were printed using an 85A shore hardness TPU filament. The print parameters used to print the lattice structure were as shown in Table 2.

3.3. Integration

Figure 9. Modular design of the instrumented toy.

The instrumented toys were designed using a modular multilayered approach to decouple the sensing capabilities from the physical properties. The sensing core determines the modality of the data that can be captured, while the physical structure determines the real and perceived affordances of the toy by the infant. The risk of harm and injury to the infant is further minimised by placing the sensors and battery at the toy's core. The physical structure fabricated using non-toxic and non-combustible materials acts as a barrier. This instrumented toy design paradigm can be expanded to utilise other sensors within the sensing core enclosed by different physical structures based on the desired play and interaction style. For the set of instrumented toys to be used in the object categorisation task to assess cognitive flexibility in infants, the sensor core records motion and pressure data from which we infer the toys' sequence of touching and squeezing. The 3D-printed lattice structure defines the toy's affordance by varying the ball and cubes' colour, size, and rigidity.

Figure 10. Set of instrumented toy prototypes.

Preprints (www.preprints.org) | NOT PEER-REVIEWED | Posted: 29 December 2022 doi:10.20944/preprints202212.0554.v1

4. Squeezing Detection

4.1. Experimental Setup

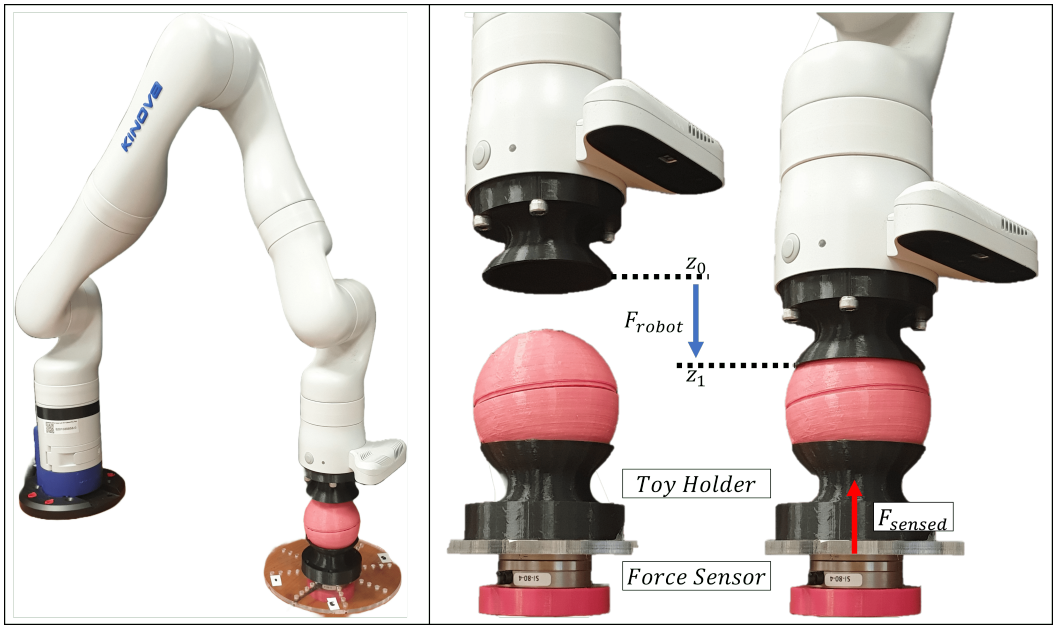

Figure 11. Kinova Gen3 7 DoF Robot applying squeezing force on instrumented toys.

A preliminary quantitative experiment to verify if the barometer of the P6 sensor embedded in each toy can detect squeezing was performed using a Kinova Gen3 7 Degree of Freedom (DoF) robotic arm (Figure 11) to repeatedly and consistently squeeze each toy ten times. An ATI Industrial Automation Net Force/Torque Sensor Mini40 was used to measure the reaction forces (F_{sensed}). A 3D printed holder was fastened to the robot end effector and force sensor to hold the toys in place and control the toy's contact area. The cubes had a contact area of 72.00 cm^2, and the balls had a contact area of 64.84 cm^2 between the robot end effector and the force sensor. It was noted that studies on infant grip force within the first 12 months had measured the range to be between 5 to 35 kPa [29,30,39,40,49]. As such, to validate performance in a minimal force application condition, the robot was programmed in position control mode to move 10 mm vertically from z_0 to z_1 with a velocity of 65 mm/s to apply a force F_{robot} = 20 N on the toys. The expected pressure applied on the cubes was 2.77 kPa and on the balls was 3.08 kPa, well under the typical grip strength range. Before beginning the experiment, each object was placed on the force sensor, and its weight was zeroed out. Data from the robot and the force sensor was timestamped and logged to a PC. The internal time of the P6 sensor was synchronised with the PC clock.

4.2. Results and Discussion

The robot consistently moves 10 mm to squeeze the toys 10 times with a regular force of F_{robot} (Figure 12).

Table 3. Squeezing Results.

Toy	Robot Applied Force (N)	Applied Pressure (Pa)	Measured Force (N)	Barometer Pressure (Pa)	% Pressure Detected
Soft Cube	20.0	2777.78	17.5 (88%)	16.04 $\pm$ 2.64	0.58%
Hard Cube	21.0	2916.67	19.0 (90%)	324.60 $\pm$ 3.62	11.13%
Soft Ball	22.0	3392.97	18.0 (82%)	51.75 $\pm$ 4.53	1.53%
Hard Ball	21.0	3238.74	18.0 (86%)	371.25 $\pm$ 5.12	11.46%

Preprints (www.preprints.org) | NOT PEER-REVIEWED | Posted: 29 December 2022 doi:10.20944/preprints202212.0554.v1

The compliance of the instrumented toy's structure produces a difference between the force applied by the robot and the force measured by the force sensor (Table 3). The soft cube absorbs 12%, the hard cube absorbs 10%, the soft ball absorbs 18%, and the hard ball absorbs 14% of the applied force. Based on the force applied by the robot and the area of contact of the 3D-printed holders, we can estimate the pressure applied to each toy when squeezing. As expected, the pressure exerted ranges from 2.77 to 3.39 kPa. This will not saturate the barometer as its specified dynamic range is 100 kPa (26 to 260 kPa).

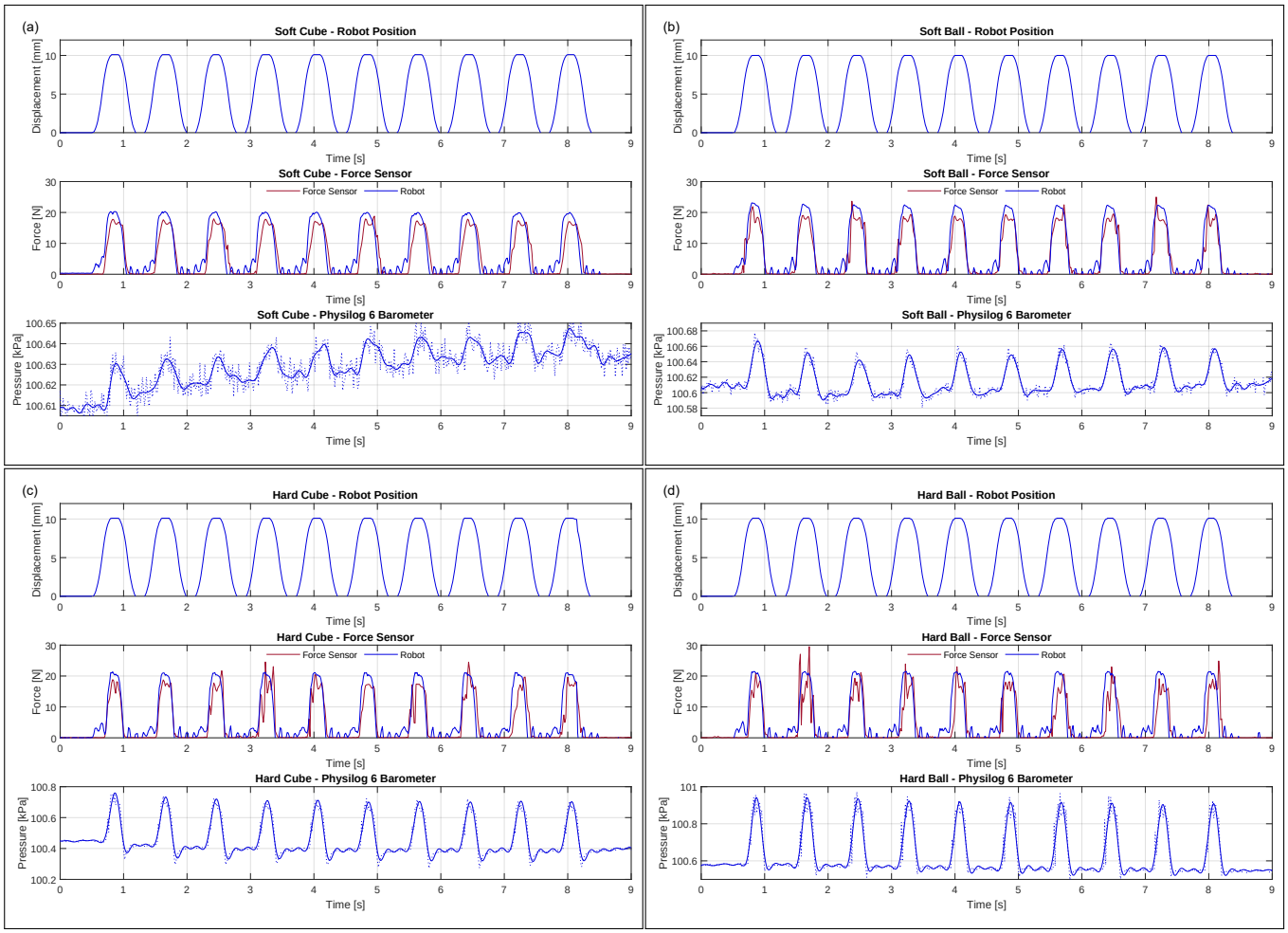

Figure 12. Barometric squeezing detection.
(a) Soft Cube (b) Soft Ball (c) Hard Cube (d) Hard Ball.

In Table 3, we can see the summary of the barometer readings across 10 squeezes for all the different toys. Noise in the barometer signal is smoothed out using a 5 Hz low-pass filter. The squeezing force applied to the toys produces a change in internal pressure that is successfully recorded by the barometer (Figure 12). The soft toys record a smaller change in pressure than the hard ones due to the compliance of the physical structure absorbing some of the force applied.

A drift in the baseline pressure reading of the barometer in the soft cube (Figure12(c)) is observed. A drift of approximately ± 20 Pa is present across all sensors either due to air leaking or getting trapped within the 3D-printed structure or the sensor core through the USB-C connector port. This drift is not of particular concern as the sensor is still able to consistently pick up on the dynamic changes in pressure caused by the actual squeezing of the toy. However, applying a 0.5 Hz high-pass filter helps filter out such a drift and the baseline offset of the ambient room pressure as well (Figure 13).

Preprints (www.preprints.org) | NOT PEER-REVIEWED | Posted: 29 December 2022 doi:10.20944/preprints202212.0554.v1

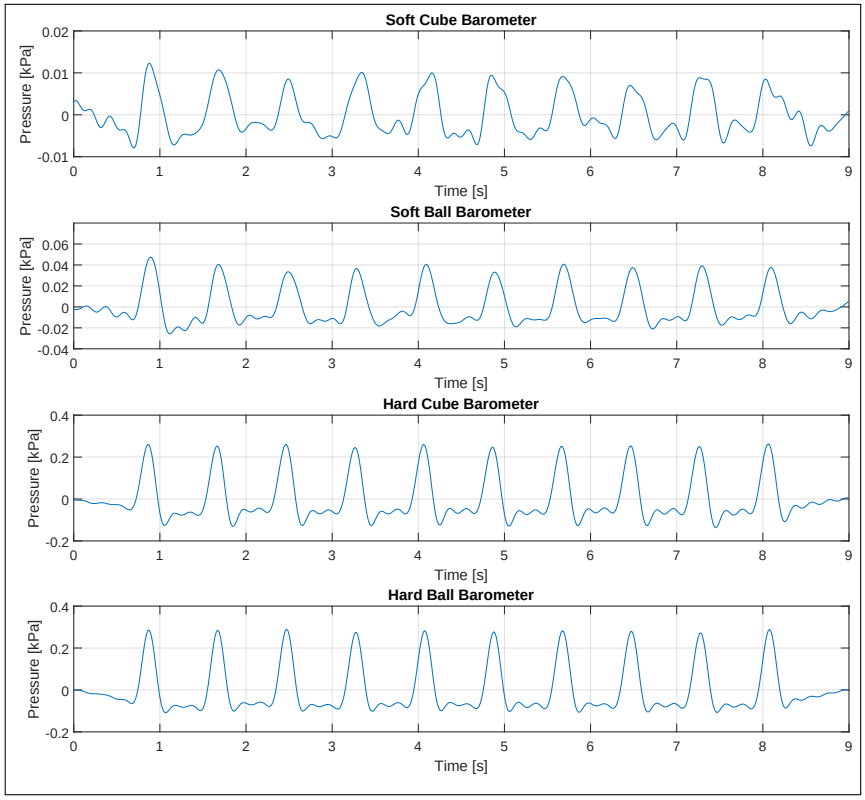

Figure 13. Filtered Barometeric Signals.

Furthermore, our barometric squeezing detection validation was based on 10% of typical infant grip pressure. The softer toys detected approximately 1% of the applied pressure, and the hard toys detected approximately 11% of the applied pressure. Therefore, we can be certain that under more representative conditions, where infants may apply 5 to 35 *kPa* of grip pressure, our novel implementation of detecting squeezing using a barometric tactile sensor will be able to detect the squeezing of the toys.

5. Sequence of Touching

5.1. Experimental Setup

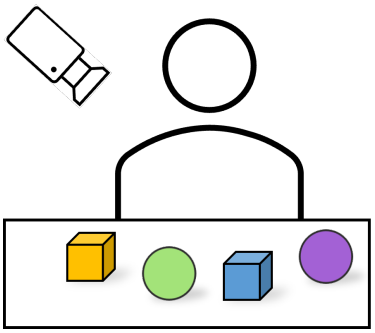

Figure 14. Sequential Touching Experiment.

A preliminary quantitative experiment was performed using the instrumented toys to detect the sequence of touching. A participant was presented with 4 instrumented toys on a table and asked to touch and play with them (Figure 14). The IMU onboard the P6 sensor embedded in each toy recorded the motion, while a camera simultaneously filmed the toy interaction from an overhead angle to minimise occlusions. The 4 IMUs and the camera were synchronised using the timestamped data from both sensors.

Preprints (www.preprints.org) | NOT PEER-REVIEWED | Posted: 29 December 2022 doi:10.20944/preprints202212.0554.v1

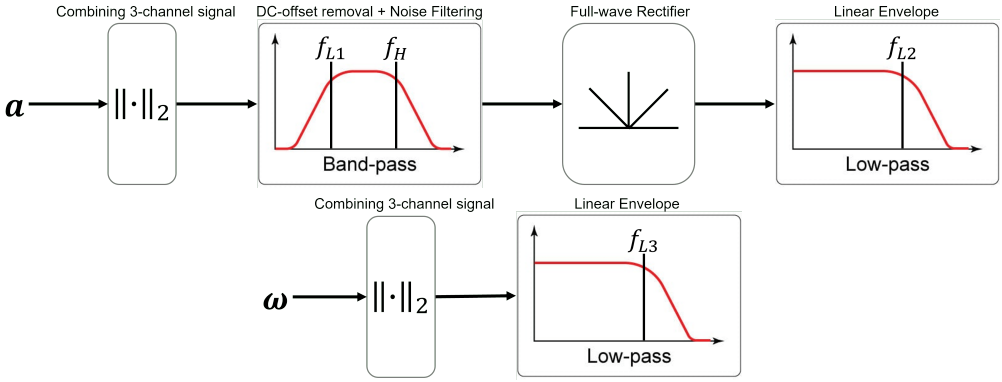

Figure 15. Accelerometer and Gyroscope signal processing.

The signals from the IMUs were processed as in Figure 15 to obtain the sequence of touching. First, the signal from the 3-channel accelerometer was combined by calculating the Euclidean norm $\|\mathbf{a}\|_2 = \sqrt{a_x^2 + a_y^2 + a_z^2}$. Then the DC-offset and noise were filtered using a band-pass filter ($f_{L,1}$ and f_H), and the signal was passed through a full-wave rectifier to get only the positive magnitude of the signal. Finally, the linear envelope was calculated using a low-pass filter ($f_{L,2}$). Similarly, the signal from the 3-channel gyroscope was combined by calculating the Euclidean norm $\|\boldsymbol{\omega}\|_2 = \sqrt{\omega_x^2 + \omega_y^2 + \omega_z^2}$, and the linear envelope was calculated using a low-pass filter ($f_{L,3}$).

5.2. Results and Discussion

From the video, an independent rater manually coded for the sequence of touches of each toy. These results are our ground truth data for evaluating the performance of the instrumented toy (Table 4). The soft and hard cubes were touched 2 times, and the soft and hard balls were touched 3 times.

Table 4. Ground truth touch timing and sequence from video coded by a human rater.

Instrumented Toy	Touch Timing (*sec*)
Soft Cube	1.60
Hard Cube	5.30
Hard Ball	9.30
Soft Ball	12.20
Hard Ball	16.50
Hard Cube	16.60
Soft Ball	20.10
Soft Cube	20.30
Hard Ball	23.70
Soft Ball	28.20

For the accelerometer, the DC-offset and noise were filtered using $f_{L,1}$ = 0.5 Hz and f_H = 10Hz band-pass filter. The linear envelope for the accelerometer and gyroscope were calculated using a $f_{L,2}$ = 0.3 Hz and $f_{L,3}$ = 0.2 Hz low-pass filter, respectively. A threshold value of 0.046 g for the accelerometer and 65 deg/s for the gyroscope was used to identify the initial instance of touching.

From the IMU data (Figure 16), the touching sequence corresponded with the video's sequence. The timings of the touch from the video were extracted by interpolating from the frame timings as touch sometimes occurs between frames. In contrast, the timing for the IMU comes directly from the data logged with precise discrete timestamping at a high sampling frequency of 64 Hz.

Preprints (www.preprints.org) | NOT PEER-REVIEWED | Posted: 29 December 2022 doi:10.20944/preprints202212.0554.v1

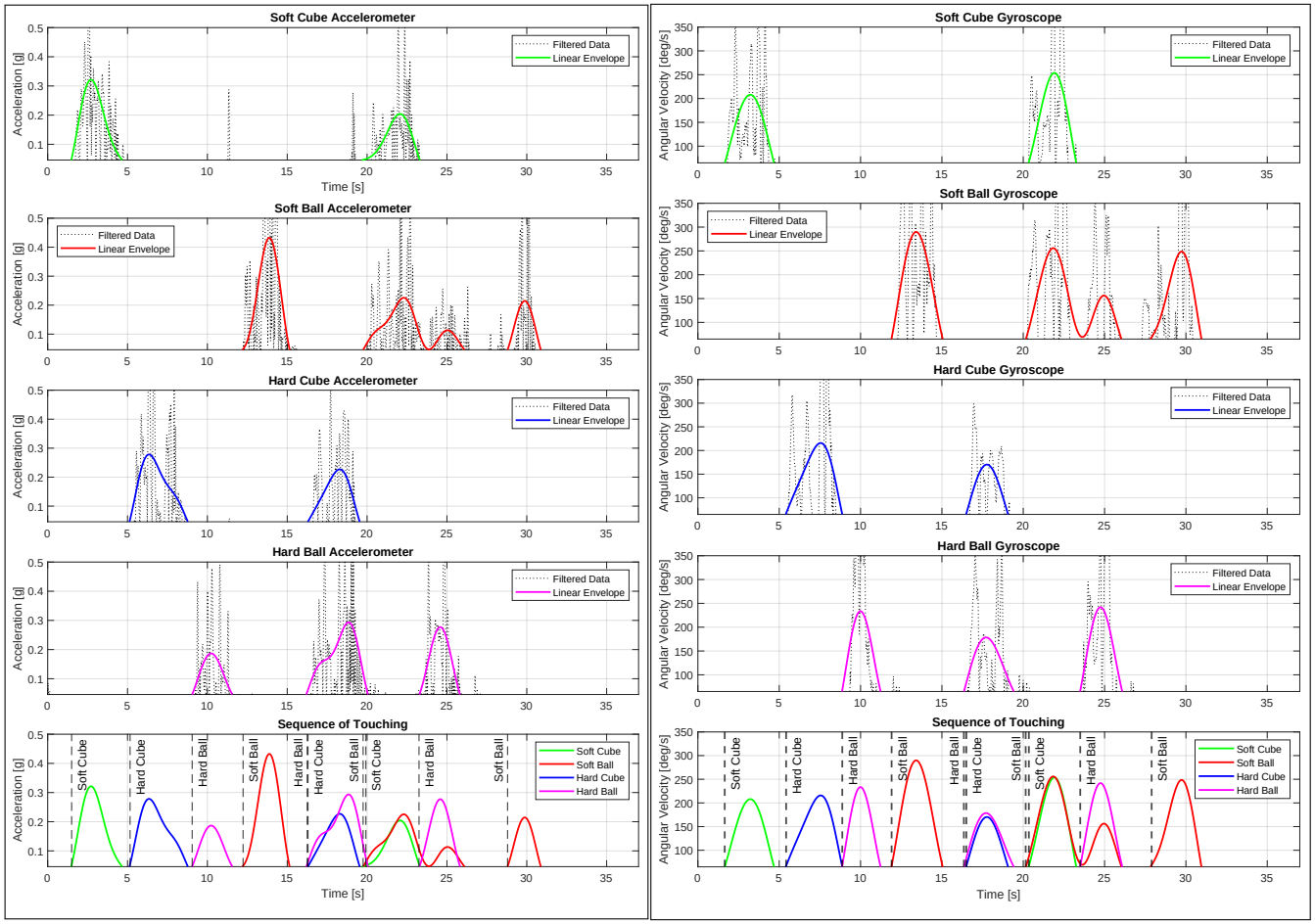

Figure 16. Accelerometer and Gyroscope data indicating sequence of touches.

Table 5. Touch sequence timing comparison.

Toy	Ground Truth (sec)	Accelerometer (sec)	Accelerometer Error	Gyroscope (sec)	Gyroscope Error	Average (sec)	Average Error
Soft Cube	1.60	1.50	-0.10	1.67	0.07	1.59	-0.01
Hard Cube	5.30	5.16	-0.14	5.42	0.12	5.29	-0.01
Hard Ball	9.30	9.06	-0.24	8.87	-0.43	8.97	-0.33
Soft Ball	12.20	12.20	0.00	11.91	-0.29	12.06	-0.14
Hard Ball	16.50	16.25	-0.25	16.35	-0.15	16.3	-0.20
Hard Cube	16.60	16.30	-0.30	16.50	-0.10	16.4	-0.20
Soft Ball	20.10	19.75	-0.35	20.18	0.08	19.97	-0.13
Soft Cube	20.30	19.92	-0.38	20.35	0.05	20.14	-0.16
Hard Ball	23.70	23.30	-0.40	23.50	-0.20	23.4	-0.30
Soft Ball	28.20	28.80	0.60	27.83	-0.37	28.32	0.12
RMSE	—	—	0.32	—	0.23	—	0.19

To quantify the accuracy of the IMU results, we compute the timing error and Root Mean Squared Error (RMSE) (Table 5). The accelerometer tends to estimate the touch time to be earlier than it is and has an RMSE of 0.32 seconds, and the gyroscope does a better job at estimating the touch timing with an RMSE of 0.23 seconds. We can further improve the IMU-based touch detection accuracy by taking the average touch time from the accelerometer and gyroscope, resulting in an RMSE of just 0.19 seconds.

Therefore, IMU-based touch detection is an accurate way to detect touching and interaction with the toys, removing the subjectivity of manual human coders. However, to ensure maximum accuracy and robustness, rather than entirely replacing manually coded

data with IMU-based touch detection, the human coders can leverage the IMU data to speed up the manual coding process. In a video recorded at 30 frames per second (fps), the instrumented toys can help narrow down the video to a segment spanning approximately 6 to 10 frames to confirm the exact touch time rather than go through the entire video.

6. Future Work and Conclusion

In this paper, we presented a set of instrumented toys that can be used in lab-based and ecological environments to study the development of cognitive flexibility, an aspect of EF, in infants. The toys can detect periods of motion to determine when they are touched. From this, the overall sequence of touching can be inferred to calculate MRL and the conditional probability of infant touch sequence to identify mental set-shifting. The toys can also detect when and how much they have been squeezed to further validate infants' change in mental classification from shape-based to material-based classification. To improve the sensitivity of the squeezing detection, we aim to enhance the seal around the barometer by vacuum degassing the sensor core before fully curing it to remove any air pockets. The interface between the 2 halves of the 3D-printed physical structure will also be sealed tightly. In conclusion, although the sequence of touching and squeezing was detected through preliminary tests, such results confirm the hypothesis that these instrumented toys could be helpful for quantitative monitoring and measurement of infants' EF development and are ready to be evaluated through appropriate clinical trials.

Author Contributions: "Conceptualization, V.R., M.Z.A., G.G.D., G.G.L., M.A.R., T.X.X., Y.W.Y., J.P.O., V.L., D.C.; Data curation, V.R., M.Z.A.; Formal analysis, V.R.; Methodology, V.R., M.Z.A., G.G.D., G.G.L., M.A.R., T.X.X., Y.W.Y., V.L., and D.C.; Resources, V.R., M.Z.A., M.A.R., G.G.D., G.G.L., and T.X.X; Software, V.R.; Supervision, Y.W.Y, V.L., and D.C.; Validation, V.R., M.Z.A., and D.C.; Visualization, V.R.; Writing—original draft, V.R., V.L., and D.C.; Writing—review and editing, V.R., M.Z.A., G.G.D., G.G.L., M.A.R., T.X.X., Y.W.Y., J.P.O., V.L., D.C. All authors have read and agreed to the published version of the manuscript."

Funding: This work is supported by funding from the Wellcome Leap 1kD Program.

Institutional Review Board Statement: Ethical approval for this work was obtained from the Nanyang Technological University Institutional Review Board (IRB-2022-294).

Informed Consent Statement: Appropriate consent was obtained from participants

Data Availability Statement: The data presented in this study is available on request.

Acknowledgments: The authors would like to acknowledge the support of the broader Wellcome LEAP Programme, members of the Robotics Research Center, Baby-LINC Lab and Dr Sri Harsha Turlapati. This work was also supported by the Singapore Centre for 3D Printing, Nanyang Technological University, Singapore, through the use of its additive manufacturing facilities.

Conflicts of Interest: The authors declare no conflict of interest. The funder had no role in the design of the study; in the collection, analysis, or interpretation of data; in the writing of the manuscript, or in the decision to publish the results.

References

1. Diamond, A. Executive Functions. *Annual Review of Psychology* **2013**, *64*, 135–168, [https://doi.org/10.1146/annurev-psych-113011-143750]. PMID: 23020641, https://doi.org/10.1146/annurev-psych-113011-143750.
2. Deak, G.O. The Growth of Flexible Problem Solving: Preschool Children Use Changing Verbal Cues to Infer Multiple Word Meanings. *Journal of Cognition and Development* **2000**, *1*, 157–191, [https://doi.org/10.1207/S15327647JCD010202]. https://doi.org/10.1207/S15327647JCD010202.
3. Hughes, C.; Ensor, R. Executive Function and Theory of Mind: Predictive Relations From Ages 2 to 4. *Developmental psychology* **2007**, *43*, 1447–1459. https://doi.org/10.1037/0012-1649.43.6.1447.
4. Anderson, P. Assessment and Development of Executive Function (EF) During Childhood. *Child Neuropsychology* **2002**, *8*, 71–82, [https://doi.org/10.1076/chin.8.2.71.8724]. PMID: 12638061, https://doi.org/10.1076/chin.8.2.71.8724.
5. Gündüz, B. Emotional intelligence, cognitive flexibility and psychological symptoms in pre-service teachers. *Educational Research Review* **2013**, *8*, 1048–1056. https://doi.org/10.5897/ERR2013.1493.

6. Stahl, L.; Pry, R. Attentional flexibility and perseveration: Developmental aspects in young children. *Child neuropsychology : a journal on normal and abnormal development in childhood and adolescence* **2005**, *11*, 175–189. https://doi.org/10.1080/092970490911315.
7. Buttelmann, F.; Karbach, J. Development and Plasticity of Cognitive Flexibility in Early and Middle Childhood. *Frontiers in Psychology* **2017**, *8*, 1040. https://doi.org/10.3389/fpsyg.2017.01040.
8. Miyake, A.; Friedman, N. The Nature and Organization of Individual Differences in Executive Functions: Four General Conclusions. *Current directions in psychological science* **2012**, *21*, 8–14. https://doi.org/10.1177/0963721411429458.
9. Ellis, A.; Oakes, L. Infants flexibly use different dimensions to categorize objects. *Developmental psychology* **2006**, *42*, 1000–1011. https://doi.org/10.1037/0012-1649.42.6.1000.
10. Mareschal, D.; Quinn, P.C. Categorization in infancy. *Trends in Cognitive Sciences* **2001**, *5*, 443–450. https://doi.org/https://doi.org/10.1016/S1364-6613(00)01752-6.
11. Mandler, J.M.; Fivush, R.; Reznick, J.S. The development of contextual categories. *Cognitive Development* **1987**, *2*, 339–354. https://doi.org/https://doi.org/10.1016/S0885-2014(87)80012-6.
12. Separating the sheep from the goats: Differentiating global categories. *Cognitive Psychology* **1991**, *23*, 263–298. https://doi.org/https://doi.org/10.1016/0010-0285(91)90011-C.
13. Ricciuti, H.N. Object Grouping and Selective Ordering Behavior in Infants 12 to 24 months old. *Merrill-Palmer Quarterly of Behavior and Development* **1965**, *11*, 129–148.
14. Horst, J.; Ellis, A.; Samuelson, L.; Trejo, E.; Worzalla, S.; Peltan, J.; Oakes, L. Toddlers Can Adaptively Change How They Categorize: Same Objects, Same Session, Two Different Categorical Distinctions. *Developmental science* **2009**, *12*, 96–105. https://doi.org/10.1111/j.1467-7687.2008.00737.x.
15. Rakison, D.; Butterworth, G. Infants' attention to object structure in early categorization. *Developmental Psychology* **1998**, *34*, 1310–1325. https://doi.org/10.1037/0012-1649.34.6.1310.
16. Welch, G.; Foxlin, E. Motion tracking: No silver bullet, but a respectable arsenal. *IEEE Computer graphics and Applications* **2002**, *22*, 24–38.
17. Campolo, D.; Taffoni, F.; Schiavone, G.; Formica, D.; Guglielmelli, E.; Keller, F. Neuro-Developmental Engineering: towards Early Diagnosis of Neuro-Developmental Disorders. In *New Developments in Biomedical Engineering*; Campolo, D., Ed.; IntechOpen: Rijeka, 2010; chapter 35. https://doi.org/10.5772/7595.
18. Luo, W.; Xing, J.; Milan, A.; Zhang, X.; Liu, W.; Kim, T.K. Multiple object tracking: A literature review. *Artificial Intelligence* **2021**, *293*.
19. Cao, Z.; Hidalgo, G.; Simon, T.; Wei, S.E.; Sheikh, Y. OpenPose: Realtime Multi-Person 2D Pose Estimation Using Part Affinity Fields. *IEEE Transactions on Pattern Analysis and Machine Intelligence* **2021**, *43*, 172 – 186.
20. Redmon, J.; Divvala, S.; Girshick, R.; Farhadi, A. You only look once: Unified, real-time object detection. 2016, Vol. 2016-December, p. 779 – 788.
21. Campolo, D.; Taffoni, F.; Formica, D.; Schiavone, G.; Keller, F.; Guglielmelli, E. Inertial-magnetic sensors for assessing spatial cognition in infants. *IEEE transactions on biomedical engineering* **2011**, *58*, 1499–1503.
22. Campolo, D.; Taffoni, F.; Formica, D.; Iverson, J.; Sparaci, L.; Keller, F.; Guglielmelli, E. Embedding inertial-magnetic sensors in everyday objects: Assessing spatial cognition in children. *Journal of integrative neuroscience* **2012**, *11*, 103–116.
23. Bondioli, M.; Chessa, S.; Narzisi, A.; Pelagatti, S.; Zoncheddu, M. Towards motor-based early detection of autism red flags: enabling technology and exploratory study protocol. *Sensors* **2021**, *21*, 1971.
24. Chi, C.; Sun, X.; Xue, N.; Li, T.; Liu, C. Recent progress in technologies for tactile sensors. *Sensors* **2018**, *18*, 948.
25. Peng, Y.; Yang, N.; Xu, Q.; Dai, Y.; Wang, Z. Recent advances in flexible tactile sensors for intelligent systems. *Sensors* **2021**, *21*, 5392.
26. Anwer, A.H.; Khan, N.; Ansari, M.Z.; Baek, S.S.; Yi, H.; Kim, S.; Noh, S.M.; Jeong, C. Recent advances in touch sensors for flexible wearable devices. *Sensors* **2022**, *22*, 4460.
27. Campolo, D.; Maini, E.S.; Patane, F.; Laschi, C.; Dario, P.; Keller, F.; Guglielmelli, E. Design of a sensorized ball for ecological behavioral analysis of infants. In Proceedings of the Proceedings 2007 IEEE International Conference on Robotics and Automation. IEEE, 2007, pp. 1529–1534.
28. Bloor, D.; Graham, A.; Williams, E.; Laughlin, P.; Lussey, D. Metal–polymer composite with nanostructured filler particles and amplified physical properties. *Applied physics letters* **2006**, *88*, 102103.
29. Cecchi, F.; Serio, S.; Del Maestro, M.; Laschi, C.; Dario, P. Design and development of sensorized toys for monitoring infants' grasping actions. In Proceedings of the 2010 3rd IEEE RAS & EMBS International Conference on Biomedical Robotics and Biomechatronics. IEEE, 2010, pp. 247–252.
30. Serio, S.M.; Cecchi, F.; Assaf, T.; Laschi, C.; Dario, P. Design and development of a sensorized wireless toy for measuring infants' manual actions. *IEEE Transactions on neural systems and rehabilitation engineering* **2013**, *21*, 444–453.
31. Tenzer, Y.; Jentoft, L.P.; Howe, R.D. Inexpensive and easily customized tactile array sensors using MEMS barometers chips. *IEEE R&A Magazine* **2012**, *21*, 2013.
32. Jentoft, L.P.; Tenzer, Y.; Vogt, D.; Liu, J.; Wood, R.J.; Howe, R.D. Flexible, stretchable tactile arrays from MEMS barometers. In Proceedings of the 2013 16th International Conference on Advanced Robotics (ICAR). IEEE, 2013, pp. 1–6.
33. Takktile sensors, Righthand Labs.

34. Ades, C.; Gonzalez, I.; AlSaidi, M.; Nojoumian, M.; Bai, O.; Aravelli, A.; Lagos, L.; Engeberg, E.D. Robotic Finger Force Sensor Fabrication and Evaluation Through a Glove. In Proceedings of the Proceedings. Florida Conference on Recent Advances in Robotics. NIH Public Access, 2018, Vol. 2018, p. 60.
35. Kõiva, R.; Schwank, T.; Walck, G.; Meier, M.; Haschke, R.; Ritter, H. Barometer-based tactile skin for anthropomorphic robot hand. In Proceedings of the 2020 IEEE/RSJ International Conference on Intelligent Robots and Systems (IROS). IEEE, 2020, pp. 9821–9826.
36. Takada, R.; Lin, W.; Ando, T.; Shizuki, B.; Takahashi, S. A Technique for Touch Force Sensing using a Waterproof Device's Built-in Barometer. In Proceedings of the Proceedings of the 2017 CHI Conference Extended Abstracts on Human Factors in Computing Systems, 2017, pp. 2140–2146.
37. Quinn, P. Estimating touch force with barometric pressure sensors. In Proceedings of the Proceedings of the 2019 CHI Conference on Human Factors in Computing Systems, 2019, pp. 1–7.
38. Taffoni, F.; Formica, D.; Campolo, D.; Keller, F.; Guglielmelli, E. Block-box instrumented toy: a new platform for assessing spatial cognition in infants. In Proceedings of the 2009 Annual International Conference of the IEEE Engineering in Medicine and Biology Society. IEEE, 2009, pp. 210–213.
39. Serio, S.; Cecchi, F.; Boldrini, E.; Laschi, C.; Sgandurra, G.; Cioni, G.; Dario, P. Instrumented toys for studying power and precision grasp forces in infants. In Proceedings of the 2011 Annual International Conference of the IEEE Engineering in Medicine and Biology Society. IEEE, 2011, pp. 2017–2020.
40. Cecchi, F.; Sgandurra, G.; Mihelj, M.; Mici, L.; Zhang, J.; Munih, M.; Cioni, G.; Laschi, C.; Dario, P. CareToy: an intelligent baby gym: home-based intervention for infants at risk for neurodevelopmental disorders. *Ieee robotics & automation magazine* **2016**, *23*, 63–72.
41. Sgandurra, G.; Beani, E.; Inguaggiato, E.; Lorentzen, J.; Nielsen, J.B.; Cioni, G. Effects on parental stress of early home-based caretoy intervention in low-risk preterm infants. *Neural Plasticity* **2019**, *2019*.
42. Digital assessments for movement and cognition. - mindmaze.com. https://www.mindmaze.com/digital-assessments-for-movement-cognition/#physilog.
43. Physilog - Gait Up | Make sense of motion - physilog.com. https://physilog.com/.
44. User Manual - Gait Up Research. https://research.gaitup.com/wp-content/uploads/2021/01/P6S_Instructions-for-Use_V1.0.0.pdf.
45. Goh, G.L.; Agarwala, S.; Yeong, W.Y. 3D printing of microfludic sensor for soft robots: a preliminary study in design and fabrication. In Proceedings of the Proceedings of the 2nd International Conference on Progress in Additive Manufacturing (Pro-AM 2016). p177–81, 2016.
46. Luis, E.; Pan, H.M.; Sing, S.L.; Bastola, A.K.; Goh, G.D.; Goh, G.L.; Tan, H.K.J.; Bajpai, R.; Song, J.; Yeong, W.Y. Silicone 3D printing: process optimization, product biocompatibility, and reliability of silicone meniscus implants. *3D Printing and Additive Manufacturing* **2019**, *6*, 319–332.
47. Goh, G.D.; Sing, S.L.; Lim, Y.F.; Thong, J.L.J.; Peh, Z.K.; Mogali, S.R.; Yeong, W.Y. Machine learning for 3D printed multi-materials tissue-mimicking anatomical models. *Materials & Design* **2021**, *211*, 110125.
48. Goh, G.D.; Goh, G.L.; Lyu, Z.; Ariffin, M.Z.; Yeong, W.Y.; Lum, G.Z.; Campolo, D.; Han, B.S.; Wong, H.Y.A. 3D Printing of Robotic Soft Grippers: Toward Smart Actuation and Sensing. *Advanced Materials Technologies* **2022**, *7*, 2101672.
49. Upshaw, M.B.; Bernier, R.A.; Sommerville, J.A. Infants' grip strength predicts mu rhythm attenuation during observation of lifting actions with weighted blocks. *Developmental Science* **2016**, *19*, 195–207.